Vol. 24, No. 2(2025) Mat25444
Revista Mexicana de Ingeniería Química

# Molecular dynamics of SDS-coated gold nanoparticles in aqueous medium with Coarse-grained model and MARTINI force field

# Dinámica molecular de nanopartículas de oro recubiertas con SDS en medio acuoso con modelo Coarse-grained y campo de fuerza MARTINI

D.E. Altamirano-Bulnes*, E.D. Estrada-López
Departamento de Ingeniería Química. Universidad Nacional Autónoma de Honduras, Tegucigalpa, Francisco Morazán, Honduras.
Received: October 17, 2024; Accepted: April 8, 2025

## Abstract
Gold nanoparticles have garnered significant interest in recent years across various fields of study, including materials science, biomedicine, drug delivery design, electronics, and optics, among others. Numerous studies have aimed to visualize their properties by coating them with polymers, proteins, surfactants, and genes to observe and analyze variations in their functioning. With advances in computing, these nanoparticles have been examined using molecular dynamics methodologies to simulate their interactions with different solvents and particles, thereby predicting their behavior in diverse applications. In this research, spherical gold nanoparticle systems with a radius of 1.5 nm, coated with the surfactant sodium dodecyl sulfate (SDS), are investigated in an aqueous medium with varying concentrations utilizing molecular dynamics with a coarse-grained approach and the MARTINI force field to examine energy, structural, transport, and stability aspects properties.
*Keywords*: metal nanoparticles, active agent, interface, computer simulation, nanomaterials.

## Resumen
Las nanopartículas de oro han cobrado en los últimos años un gran interés en diversos campos de estudio, entre ellos: la ciencia de materiales, la biomedicina, el diseño de transporte de fármacos, la electrónica, la óptica, entre otros. Diversos estudios han buscado visualizar sus propiedades al recubrirlas con polímeros, proteínas, surfactantes y genes con el fin de observar y estudiar las variaciones en su funcionamiento. Debido a los avances en el área de la computación, este tipo de nanopartículas se han estudiado a través de la metodología de dinámica molecular con el fin de simular sus interacciones con diversos disolventes y otras partículas, para predecir su comportamiento en diferentes aplicaciones. En esta investigación se estudian sistemas de nanopartícula de oro esférica con un radio de 1.5 nm recubiertas del surfactante dodecilsulfato sódico (SDS) en un medio acuoso a través de la dinámica molecular con enfoque de coarse-grained y campo de fuerza MARTINI para analizar propiedades de energía, estructurales, de transporte y de estabilidad.
*Palabras clave*: nanopartículas de metal, agente activo, interfase, simulaciones computacionales, nanomateriales.

*Corresponding author. *E-mail*: d.bulnes97.db@gmail.com ;
https://doi.org/10.24275/rmiq/Mat25444
*ISSN*:1665-2738, *issn-e*: 2395-8472

# 1 Introduction

Nanomaterials are defined as particles that form crystals, with structures depending on the synthesis method, the surface area of the nanoparticle, and the intended final application. Their dimensions range from 1 nm to 100 nm (Khan *et al*., 2019). These versatile materials can create structural systems in materials science, enabling the characterization of electronic, photochemical, electrochemical, optical, magnetic, catalytic, and mechanical properties that differ significantly from those of macro systems. (Khan *et al*., 2019). This difference has led to a growing interest in nanomaterials in recent years, particularly in metals that interact with various electronic, photochemical, electrochemical, catalytic, and mechanical systems. One metal that has attracted attention due to technological advances in materials science at both macro and nano scales is gold. Gold nanoparticles (AuNPs) have numerous applications in the medical field, especially in the transport of drugs, genes, and proteins; treatments for tumors and cancer cells through photothermal therapy (PTT), photodynamic therapy (PDT), radiative therapy (RT), and imaging via X-ray and computed tomography (Hu *et al*., 2020; Ramalingam, 2019). Moreover, due to their diverse characteristics and modifications, AuNPs are significantly interesting in various multidisciplinary fields, such as chemical and biological labeling, gaseous labeling, $CO_2$ capture, and other important applications (Barrak *et al*., 2016; Ganesh *et al*., 2013; I. Khan *et al*., 2017; Lee *et al*., 2011; Mansha *et al*., 2017; Montoya-Villegas *et al*., 2020; Nuñez-Delgado *et al*., 2023; Ramacharyuly, P. V. R. K.; Muhammad, Raeesh; Kumar, Praveen J.; Prasad, 2015; Rawal & Kaur, 2013; Shaalan et al., 2016; Velasco-Rodriguez *et al*., 2012).

For decades, ligands like oligonucleotides, drugs, peptides, and conjugated polymers have been used to bind to AuNPs via thiol group bonds, aiming to support and protect these structures (Asish, Pal; Aasheesh & Bhattacharya, 2009; Lu *et al*., 2014; Si *et al*., 2018). The AuNPs are anchored to the ligands of interest through covalent and non-covalent interactions, which, under specific pH or salt conditions, facilitate the release of these particles in targeted areas via in-solution injection (Applications, 2017). Notably, one of the most frequently used ligands is sodium dodecyl sulfate (SDS), a surfactant that transforms the properties of interfaces. Its characteristics have been extensively studied, making it a suitable candidate for various applications in materials science in conjunction with gold nanoparticles.

Molecular dynamics studies have been conducted using various coatings for AuNPs. (Elahi *et al*., 2018). Due to the high computational cost of all-atom simulations, the coarse-grained approach, which involves packing individual chemical structures into larger assemblies, offers an appealing method for mesoscale modeling. This is because it significantly extends simulation times and the average size of study systems from nanometers to micrometers. Coarse-grained molecular dynamics (CGMD) uses a mapping technique that groups together functional groups of three to five atoms, along with their hydrogens, into beads or spheres that interact with each other. (Marrink *et al*., 2007). These beads indicate the degree of polarity and affinity between chemical groups, excluding specific interactions like hydrogen bonds. The greatest advantage of this approach is that it allows for longer simulation times by mapping atoms as beads, which reduces computational costs. (Marrink *et al*., 2007).

Additionally, the coarse-grained methodology in molecular dynamics has established itself as an essential tool for studying complex biological systems and complex materials in the field of nanomaterials (Joshi & Deshmukh, 2021; Kmiecik *et al*., 2016). The methodology has allowed the modeling of systems such as pulmonary surfactant, lipid membranes, surfactant self-assembly, or membrane characterization with favorable results for the research of biomolecules or potential uses in industry (Baoukina *et al*., 2017; Estrada-López *et al*., 2017; Joshi & Deshmukh, 2021; Owen, 2014; Pizzirusso *et al*., 2016 Souza *et al*., 2018). Similarly, the methodology has been used during the simulation of polymers in solution and in the study of their mechanical properties, as in the case of poly(n-isopropylacrylamide) (PNIPAM) or polyacrylic acid (PAA); models that, through CGMD, allowed the study of their complex structures and sensitivity to temperature changes (Abu Samah & Heard, 2014; Baranowska-Korczyc *et al*., 2019; Deshmukh *et al*., 2009).

In this research, the interactions of AuNPs coated with SDS in an aqueous medium will be studied using CGMD and Newtonian dynamics in two separate systems: one with a single nanoparticle and the other with three nanoparticles, aiming to examine their energy, structural, transport, and stability properties.

# 2 Methodology

## *2.1 General conditions*

In this work, a coarse-grained model utilizing the MARTINI force field version 2.1 (Marrink *et al*., 2007; Marrink & Tieleman, 2013) was employed to simulate the interactions of gold nanoparticles coated with SDS in an aqueous system. This enables

longer simulation times with extended time steps, ranging from 10 to 50 fs, in contrast to the time steps used in all-atom molecular dynamics, which simulate each atom-atom interaction, ranging from 1 to 2 fs (Fitzgerald *et al*. al., 2015). The GROMACS computational package version 2021.4 was utilized (Abraham et al., 2015; Pronk *et al*., 2013) for system construction, molecular dynamics simulations, and analysis. The minimization of energy for the relaxation of the molecules was done using the steepest descent method (Alexander, 1986). at 100 kJ/mol. Molecular dynamics simulations were performed using the leap-frog algorithm (Hockney *et al*., 1974; Taylor et al., 2007). For temperature balance, an NVT assembly was used using the V-rescale thermostat (Bussi *et al*., 2007). The integration time for all simulations was 20 fs. A cutoff radius of 1.2 nm was used for all nonbonding, van der Waals, and electrostatic interactions. The Lennard-Jones potential was gently delocalized from 0.9 to 1.2 nm to reduce noise at the cutoff radius. The Coulomb potential was smoothly delocalized from 0 to 1.2 nm. A dielectric constant of 15 was used for water, and a value of $4.5 \times 10^{-5}$ bar was used for isothermal compressibility. The cutoff radius performs an update every 10 steps of each simulation (Marrink *et al*., 2007). All snapshots were prepared using the VMD program.

## 2.2 *Parametrization*

The AuNPs-SDS model was generated by the Nano Modeler program (Franco-ulloa *et al*., 2022). A summary of the atomistic and coarse-grained structures of all the structures in this investigation is provided in Table 1.

Table 1. Coarse-grained schemes and chemical structures.

| Name | Chemical structure | Coarse grained representation |
|---|---|---|
| AuNP | Au X5 | Au |
| SDS | $SO_4$, $Na^+$, C1A, C2A, C3A | Qa (A3), C1A (A2), C2A (A1), C3A (A0) |
| Water | H—O—H | X4 W |
| Ion | | Na |

## 2.3 *AuNPs-SDS systems in aqueous medium*

The AuNPs were constructed in a spherical shape, with a radius of 1.5 nm, density of 19.3 g/cm$^3$, area density per ligand of 0.5 nm$^2$ /ligand, with bead type C5, bead radius of 0.166 nm and a force constant of 32,500 kJ/(mol-nm$^2$) for the C5-C5 interaction. Coating the AuNPs, with SDS (Wassenaar et al., 2015), parameterized with 3 C1 bead type with a charge of 0 and one Qa bead type with a charge of -1, using the Nano Modeler program (Franco-ulloa *et al*., 2022). This system can be visualized in Illustration 1. The system of a single AuNP-SDS in aqueous medium is depicted in Illustration 2, while the system of three AuNPs-SDS in aqueous medium is shown in the subsequent illustration 3.

For creating both systems, the gmx editconf program was used to establish a 12x12x12 nm box by introducing, with the gmx insert-molecules program, 10,000 water beads with a radius of 0.21 nm, which corresponds to 4 water molecules. Temperature equilibration was performed using the NVT ensemble at 298 K with a simulation time of 100 ns. Subsequently, an NPT molecular dynamic at 1 bar pressure with a simulation time of 200 ns was done using isotropic coupling and a Berendsen barostat (Berendsen, 1991). Analyses of the radial distribution function, the radius of gyration, and the mean square distance (MSD) were conducted. The latter provides information on the lateral diffusion coefficient of the nanoparticle in the aqueous medium, while thermodynamic studies offer insights into the stability of the system based on temperature, pressure, and density parameters.

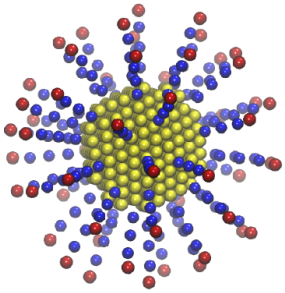

Illustration 1. Coarse-grained model of AuNP coated with SDS (AuNP-SDS). Gold nanoparticle (yellow), carbon chains of the SDS ligand (C1A-C3A) (blue) and polar head (Qa) (red).

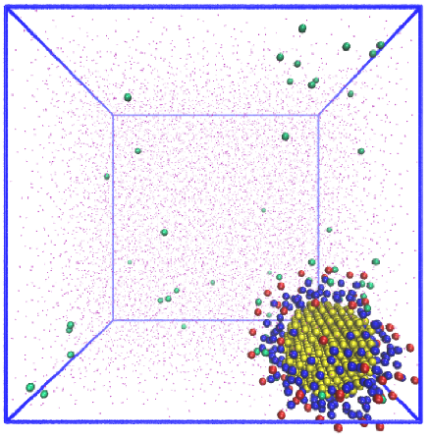

Illustration 2. Coarse-grained model of AuNP-SDS solvated in water (purple) and counterbalanced by sodium ions (green) in a 12x12x12 nm box.

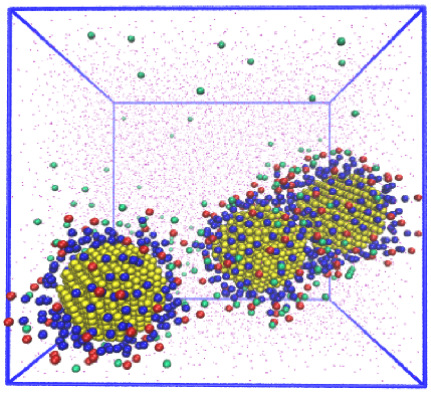

Illustration 3. Coarse-grained model of a 3 AuNPs-SDS system solvated in water (purple) and counterbalanced by sodium ions (green) in a 12x12x12nm box.

## 3 Results and discussion

### *3.1 Thermodynamics parameters*

The results of a single gold nanoparticle in an aqueous medium system (AuNP-SDS-$H_2O$) demonstrate temperature stability of (298 ± 2)K, indicating that the thermostat employed effectively maintains a consistent temperature in the system. This illustrates that the V-rescale thermostat is a well-known approximation for temperature control in the CGMD system. The experimental density of water at room temperature (25 °C) is 997.05 kg/m$^3$. Considering that the coarse-grained model overestimates the parameterization for water, the expected density at this temperature is 1000 kg/m$^3$. The AuNP-SDS-$H_2O$ system exhibits an increase in density from 1000 kg/m$^3$ to 1233 kg/m$^3$, with an uncertainty of 5 kg/m$^3$ ( 1233 ± 5) kg/m$^3$, thus demonstrating an increase of approximately 233 kg/m$^3$ resulting from the addition of the SDS-coated gold nanoparticle, which remains relatively constant throughout the simulation.

For the three gold nanoparticles in the aqueous medium system (AuNP-SDS-$H_2O$), the temperature remained constant at a value of (298 ± 2)K like that observed for the simulation of a single AuNP. The three AuNP-SDS-$H_2O$ systems show a density increase from 1000 kg/m$^3$ to 1609 kg/m$^3$, with an associated uncertainty of 3 kg/m$^3$ (1609 ± 3)kg/m$^3$; this shows an increase of approximately 609 kg/m$^3$ from the addition of three gold nanoparticles coated with SDS. When performing a simple subtraction, compared to the single AuNP-SDS-$H_2O$ system, the density difference is 376 kg/m$^3$. This suggests that each gold nanoparticle coated with the surfactant contributes to an increase of approximately 200 kg/m$^3$ in the system's density, assuming the system's density is the sum of its individual contributors.

### *3.2 Coulomb and van der Waals interaction energy*

Table 2 shows the average Coulomb ($E_C$) and van der Waals ($E_{LJ}$) interaction energies for the entire system, including AuNP-SDS-ions and AuNP-SDS-AuNP-SDS, for one and three AuNPs, measured in kJ/mol. The values presented in this table are strongly dependent on the field used, so they may vary from those of other studies. This emphasizes the importance of properly using force fields for simulations conducted with coarse-grained methodologies. Therefore, the objective of this discussion is to illustrate the trends of the simulated systems. Both the $E_C$ and $E_{LJ}$ interaction energies show an increase in energy for both whole systems; however, the $E_C$ interactions exhibit an increase of more than three times for the entire system. Conducting a more detailed analysis of the interactions between the two systems and AuNP-SDS-ions, we observe that the $E_C$ and $E_{LJ}$ energies exhibit the same trend as the whole systems, showing an increase of more than three times in their energies when transitioning from one to three AuNPs. This increase indicates a stronger attraction of the AuNP-SDS to the $Na^+$ ions as their concentration rises from one to three AuNP-SDS. In the case of the $E_C$ and $E_{LJ}$ analyses of the AuNP-SDS-AuNP-SDS interaction, it can be observed that the electrical interactions between the Au-NP-SDS are repulsive as the concentration increases and attracts through van der Waals intermolecular forces. However, the sum of $E_C$ and $E_{LJ}$ is negative, indicating a consistent tendency for AuNPs-SDS clusters to form as the concentration increases. Similar findings are presented in the following work (Bordoni & Colherinhas, 2022).

Table 2. The average interaction energy calculated for Coulomb (EC) and van der Waals (ELJ) for one and three AuNP in the whole system, including AuNP-SDS-ions and AuNP-SDS-AuNP-SDS, is presented in kJ/mol. The latter two measurements are provided per number of AuNP in an aqueous solution. RMSD values are shown for all average interactions.

| Components | 1 AuNP | 3 AuNP |
|---|---|---|
| | $E_C$ | |
| Whole system | $-870.79 \pm 36.63$ | $-2,971.33 \pm 56.89$ |
| AuNP-SDS-ions | $-659.09 \pm 45.84$ | $-2,621.94 \pm 77.99$ |
| AuNP-SDS-AuNP-SDS | - | $31.14 \pm 30.36$ |
| | $E_{LJ}$ | |
| Whole system | $-316,540 \pm 499$ | $-374,201 \pm 540$ |
| AuNP-SDS-ions | $-406.90 \pm 46.23$ | $-1,565.79 \pm 78.50$ |
| AuNP-SDS-AuNP-SDS | - | $-76,039.5 \pm 145.61$ |

Nonetheless, this also suggests that if the electrical force increases significantly, the AuNPs-SDS could experience repulsion.

### *3.3 Lateral diffusion*

Lateral diffusion is an important dynamic property that measures a system's ability to move through a medium. The lateral diffusion coefficient can be calculated using Einstein's relation through the calculation of the mean square distance (MSD) of a set of atoms at specific positions. The MSD quantifies the deviation between a particle's position and its reference position. The lateral diffusion coefficient can be derived through linear regression by the least squares method, as represented by the equation:

$$\langle \|r(t) - r(t=0)\|^2 \rangle = 2Dt \tag{1}$$

Where $r(t)$is the position of the center of mass in the $xy$ plane at a time $t$, $r(t = 0)$ is the position of the center of mass at an initial time 0, and $D$ is the lateral diffusion coefficient.

In the lateral diffusion study, all data was collected from start to finish. To compare with experimental values or atomistic simulations, a conversion factor of 4 must be applied to the diffusion coefficient obtained from a simulation conducted in coarse-grained. The objective of this factor is to compensate for the faster diffusion in the coarse-grained model (Marrink *et al*., 2004)

The lateral diffusion coefficient is influenced by factors such as molecular size, shape, and interactions with the environment, including the solvent and other molecules present in the system. In the simulation of the single AuNP-SDS-$H_2O$ system, the MSD was examined in relation to the simulation time, revealing consistently increasing and linear behavior throughout the duration of the simulation. By performing a linear fit $MSD = 4Dt + b$, as shown in Figure 1 for both systems, it was found that the lateral diffusion coefficient in the $xy$ plane in the $z$ direction of the nanoparticle for the single AuNP-SDS-$H_2O$ system is $(5.559 \pm 0.004) \times 10^{-7}$cm$^2$/s. This value is greater than that reported by Giorgio of $1 \times 10^{-8}$cm$^2$/s for uncoated gold nanoparticles sized at 50 nm using atomistic molecular dynamics. In another study of gold nanoparticles measuring 5 nm, the experimentally reported value is $1.5 \times 10^{-9}$cm$^2$/s; this nanoparticle size would be in greater agreement with this study (Vaisey *et al*., 2022). Wong and collaborators studied the translational diffusion of gold nanoparticles in toluene and water using the dynamic light scattering technique at different temperatures. They found that for a nanoparticle with a hydrodynamic radius of 16 nm at 298 K in an aqueous medium, its diffusion coefficient is $(1.53 \pm 0.035) x 10^{-7}$cm$^2$/s, which is of the same order of magnitude as the value calculated by the simulation. Other values have been reported experimentally in various sizes, yielding comparable results. (Albaladejo *et al*., 2009; Zimbone *et al*., 2011). It is important to note that even the experimental values for the diffusion of gold nanoparticles vary depending on the technique and the objectives of the study. The variations in values may be directly attributed to the coating of the gold nanoparticle with SDS, which significantly enhances its diffusion throughout the system by lowering the surface tension of water. Furthermore, the CGMD restricts the particle's degrees of freedom. Another factor that may explain the variations is the particle size used (Wong *et al*., 2015). In a CGMD study, a diffusion coefficient of approximately value $4.0 \times 10^{-7}$cm$^2$/s for a size of 2 nm is reported. As the radius of the discovered nanoparticle increases, the diffusion coefficient decreases from $4.0 \times 10^{-7}$ cm$^2$/s to $2.0 \times 10^{-7}$cm$^2$/s. Therefore, there is a dependence on the size of the nanoparticle on its diffusion in an aqueous medium (Gupta & Rai, 2017). Regarding the three AuNPs-SDS-$H_2O$ system, it has been found that the lateral diffusion coefficient is $(7.300 \pm 0.015) x 10^{-7}$cm$^2$/s. This value is higher than that calculated for a gold nanoparticle in an

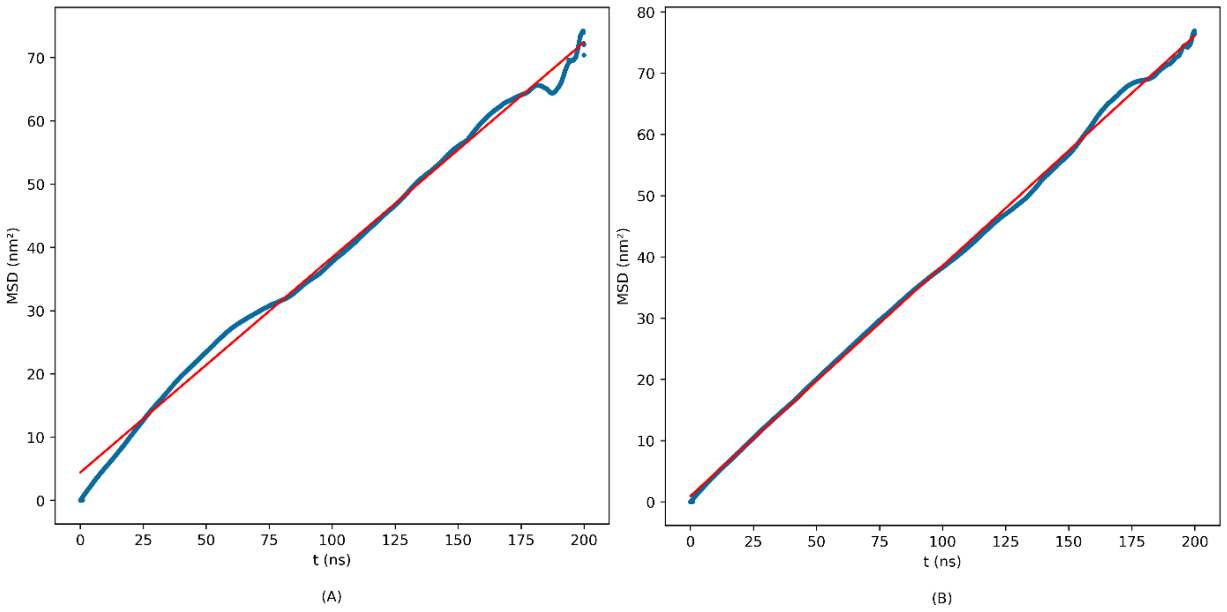


Figure 1. Comparison of linear regression for the variation of the mean square distance (MSD) throughout the simulation for one (A) and three (B) AuNPs-SDS systems in an aqueous medium. Simulated data (turquoise) and linear fit (red).

aqueous medium. This suggests that a greater number of coated nanoparticles may result in enhanced diffusion throughout the aqueous system. Subsequent simulations are needed to consider a larger number of AuNPs, which can form a bigger cluster to achieve increased diffusion.

### *3.4 Radial distribution function*

In statistical mechanics, the Radial Distribution Function (RDF) describes the spatial distribution of particles in condensed phase systems, such as liquids or solids. The RDF indicates the probability of locating a particle at a specific point in space relative to another reference particle (Harding & Harding, 2007).

Mathematically, RDF is defined as the conditional probability density of finding a particle at a distance $r$ with respect to a reference particle located at the origin within a system of particles. The RDF, denoted as $g(r)$ is defined as:

$$g(r) = \frac{1}{\langle \rho_B \rangle_{local}} \left( \frac{1}{N_A} \right) \sum_{i \in A}^{N_A} \sum_{j \in B}^{N_B} \frac{\delta\left(r_{ij} - r\right)}{4\pi r^2} \qquad (2)$$

Where $\langle \rho_B \rangle_{local}$ is the particle density of type $B$ averaged over all spheres around particles $A$ with radius $r_{\max}$, $r$ is the distance between the particles, $r_{ij}$ is the distance between the reference particle and neighboring particle i, $N_A$ is the density of the particles $A$, $N_B$ is the density of the particles $B$, and $\delta\left(r - r_{ij}\right)$ is the Dirac delta function which represents the probability of finding a particle at the distance $r$ relative to the particle reference $r_{ij}$. The sum is calculated over all neighboring particles in the system. This provides insight into the structure and organization of the particles system.

The RDF analysis referenced the water particles of the system for both the one and three AuNP-SDS systems in an aqueous medium. As shown in Figure 2, the different RDFs for the A0 to A3 beads of the single AuNP-SDS are displayed. It is visualized that the A0 bead, which is the carbon atom linked to the gold nanoparticle by disulfide bonds, has a lower probability of being closer to water particles at shorter distances, which increases as the radial distance increases. The A1, A2, and A3 beads demonstrate an increase in RDF as the radius expands. This behavior, as illustrated in the figure, indicates that the polar head (A3) of the surfactant is near the water particles, varying throughout the simulation due to the folding of the ligand. At an approximate radial distance of 0.5 nm, this indicates a probability value of approximately 2.2. In the three AuNPs-SDS-$H_2O$ systems, a similar behavior is observed for all beads, with only a smaller increase in the probability for the A3 bead, which is around 2.4 at 0.5 nm. We can see that both RDFs are remarkably similar, indicating that the cluster of three AuNPs-SDS behaves like a system of one AuNP-SDS. This can be useful because systems with more AuNPs-SDS can be treated as just one AuNP-SDS for this analysis. Regarding the folding of the tails on the nanoparticles, we observe that they attempt to stay together throughout the simulation. This approach would be beneficial for maintaining a cluster of gold nanoparticles that wish to remain united in an aqueous medium.

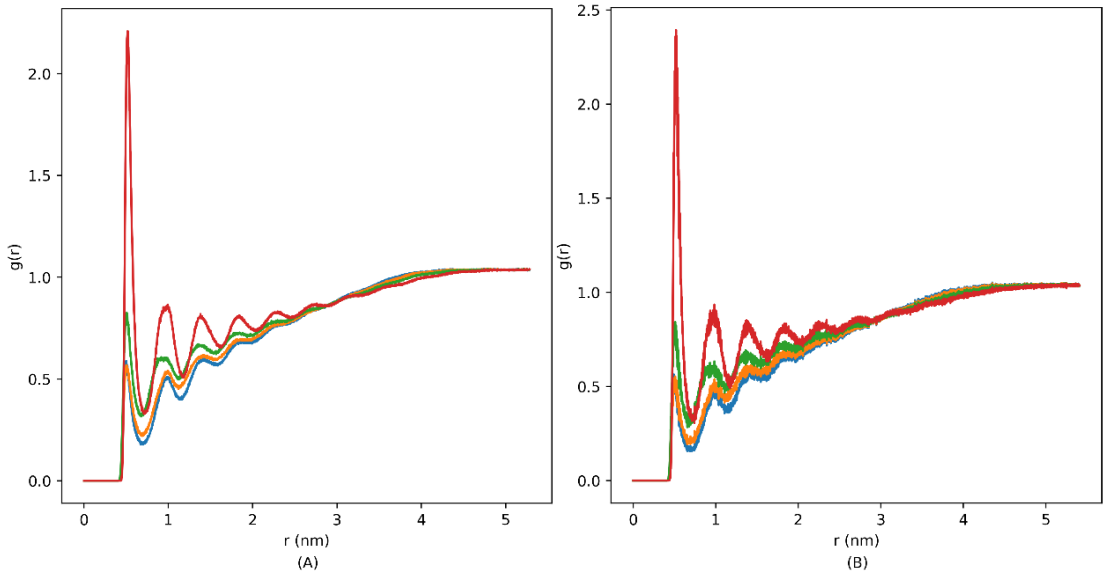


Figure 2. Comparison of RDF g(r) as a function of the nucleus radius with reference to water particles for one (A) and three (B) AuNPs-SDS systems in aqueous medium. *Bead A0* is carbon (blue), *Bead A1* is carbon (orange), *Bead A2* is carbon (green), and *Bead A3,* is polar head (red).

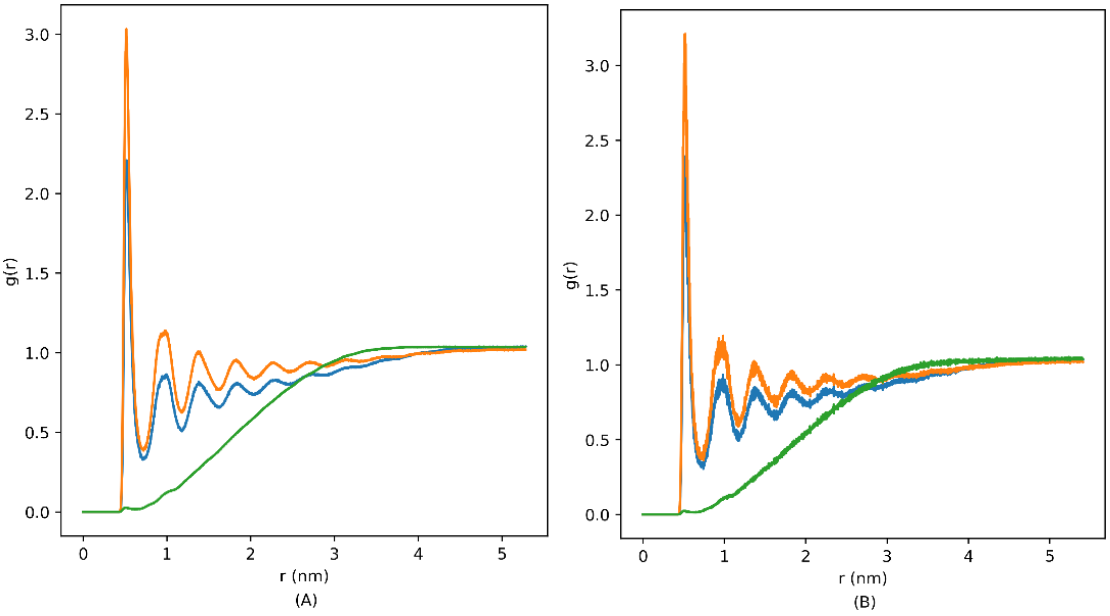


Figure 3. Comparison of the RDF g(r) for one (A) and three (B) AuNP-SDS systems with water particles as the reference. Nucleus (green), polar head (blue), and ion (orange).

Figure 3 compares the RDF of the nucleus, polar head, and ion for both AuNPs-SDS systems, using water as the reference. The ions are more likely to be near water particles than the nucleus and the polar head in both systems. Additionally, in the three AuNP-SDS systems, the slight increase in probability persists among the three references of the nucleus, the polar head, and the ion. As the concentration of AuNP-SDS increases, as seen in the energy analysis, the attraction of the sodium ions grows, imparting a polar behavior to the AuNP-SDS system compared to the uncoated AuNP, which exhibits nonpolar characteristics in the coarse-grained approach. (Marrink *et al*., 2007).

### *3.5 Gyration radius*

The radius of gyration is defined as the radial distance to a point that would possess a moment of inertia equal to that of the actual mass distribution of the body at its center of mass. This measure provides information

about the spatial distribution of mass or charge within the system, thus serving as a metric for studying the structural properties of motion objects. Formally, this is defined as the average distance of the particles in the system from their center of mass and is commonly denoted by the letter $R_g$. Mathematically, the radius of gyration can be calculated through the equation:

$$R_g = \sqrt{\frac{1}{N}\sum_{i=1}^{N}(r_i - R_{cm})^2} \tag{3}$$

where $N$ is the total number of particles in the system, $r_i$ is the coordinate of the individual particles in the system, typically represented in Cartesian coordinates, and $R_{cm}$ is the center of mass of the system, calculated as the weighted average of the particle coordinates in the system. The radius of gyration provides information about the spatial extent and shape of the entity under study. A larger value $R_g$ indicates an extended entity, while a smaller value $R_g$ indicates a more compact entity.

When performing the radius of gyration analysis on the single AuNP-SDS-$H_2O$ system, stable behavior is observed throughout the simulation time. For the nucleus, Figure 4 (A) displays an average value of (1.1172 ± 0.0006) nm. This value indicates that the nucleus of the nanoparticle does not experience a sudden conformational change during its interaction with the aqueous medium. For the ligands, the reported average value is (2.01 ± 0.01) nm, which is greater than that of the nucleus. This indicates that the SDS surfactant is spread throughout the simulation when compared to the nucleus.

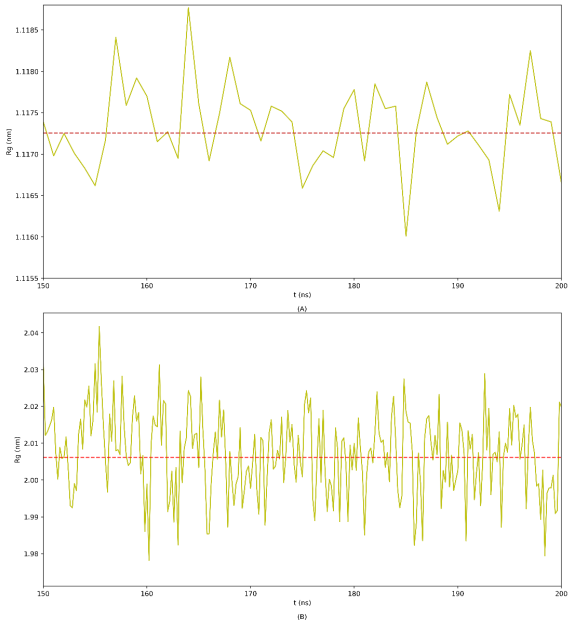


Figure 4. Values of the Rg for the nanoparticle nucleus (A) and ligands (B) throughout the simulation of the single AuNP-SDS in aqueous medium. The variation of the Rg is depicted in yellow, along with the average value of Rg shown in red.

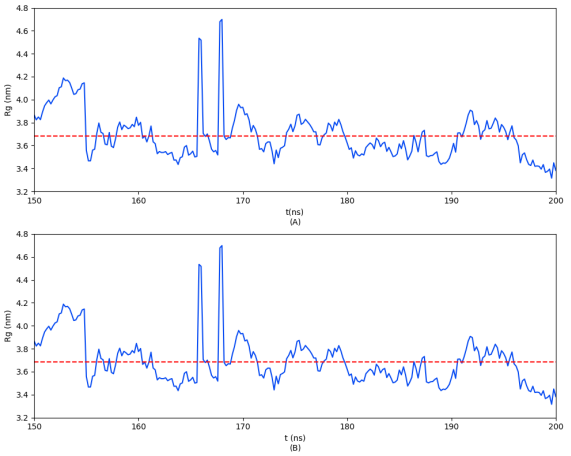


Figure 5. Values of Rg for the nanoparticle nucleus (A) and ligands (B) throughout the simulation of the three AuNPs-SDS in an aqueous medium. The variation of the Rg is depicted in blue, along with the average value of Rg shown in red.

Figure 5 displays the radius of gyration values for the nucleus and ligands in the three AuNPs-SDS systems. An average value of (3.7 ± 0.2) nm for the nucleus of the three AuNPs-SDS- $H_2O$ systems is reported. In comparison to the overall simulation duration, a decreasing trend is evident in the last nanoseconds of the simulation. This is explained by observing the trajectory of the simulation, where, initially, the three nanoparticles are randomly positioned within the box. As the simulation progresses, they become compacted and draw closer to one another, ultimately resulting in a value below 3.4 nm. Comparing this result to the single AuNP nucleus, we observe an increase in the average value that exceeds even the Rg SDS analysis. However, stability is observable in the aqueous medium with low variability. This can be interpreted to mean that nanoparticles in an aqueous medium prefer to form conglomerates rather than remain separate from one another. This behavior could be useful for agglomerating a certain number of nanoparticles that facilitate the transport of particles in various context systems. For the SDS in the tree AuNPs system, the average value reported is (3.7 ± 0.2)nm. It is observed that, similar to the nucleus, the radius of gyration of the ligands for the three AuNPs-SDS systems decreases as the three nanoparticles come closer together throughout the simulation. No differences were observed in the Rg value when we compared the nucleus and SDS in the three AuNPs-SDS systems. Indicating that the three AuNP-SDS systems offer more flexibility compared to the single one.

## *3.6 Density profile*

The density profile informs us about the local distribution of structures within the simulation

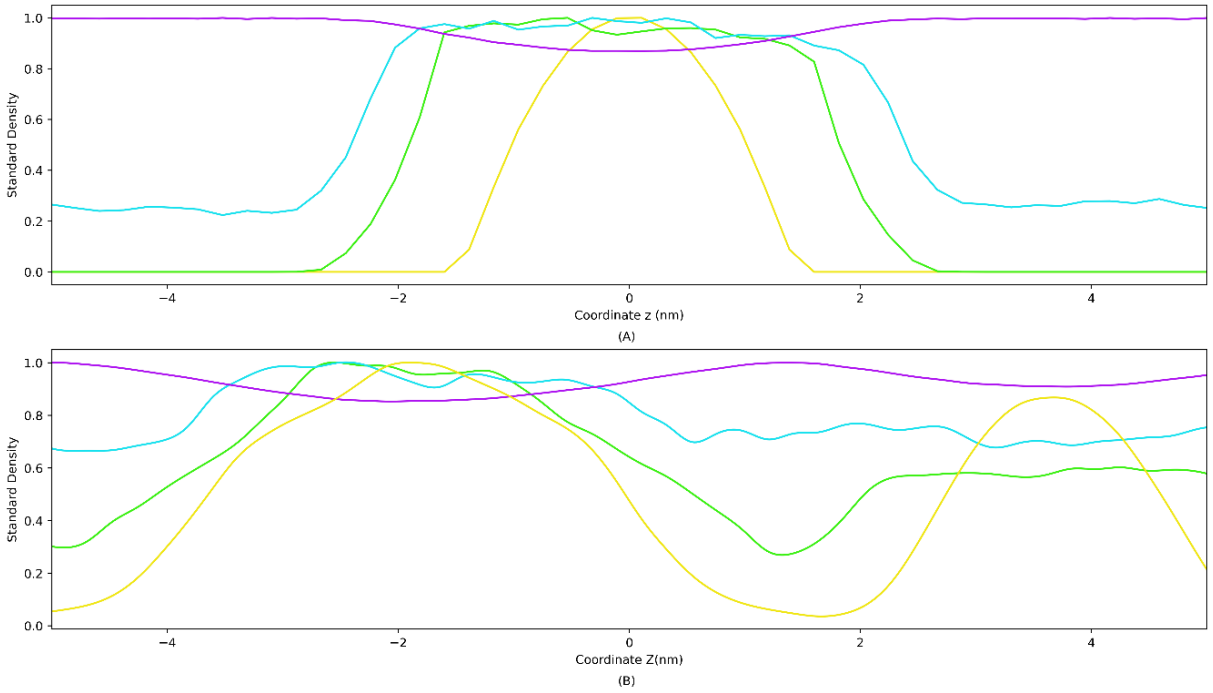


Figure 6. Density profile for one (A) and three (B) AuNPs-SDS systems in aqueous medium. Nucleus (yellow), water (purple), ion (blue), and SDS (green).

system. When analyzing the density profile for one AuNP-SDS-$H_2O$ system and three AuNPs-SDS-$H_2O$ systems, a distinction in the distribution of the components is visualized. The analysis involved standardizing all density values using the maximum value calculated in the simulation for each element: gold nucleus, SDS, ion, and water. Figure 6 shows that in the single AuNP-SDS-$H_2O$ system, the ligands are located far from the nucleus, while the ion remains within the ligands, thus supporting the neutralization of the polar head. On the other hand, in the system with three AuNP-SDS, when three gold nuclei are present, there is a higher concentration of gold nanoparticle nuclei at distances between -4 and 0 nm. This indicates that two AuNPs-SDS are present on this side of the box, compared to the other AuNP-SDS located between 2 and 4 nm, where the presence of the SDS and ions has a slight separation. This suggests that the presence of more than two AuNPs-SDS in the same system modifies the interactions of ions, SDS, and water. The AuNP-SDS on the right side of the box is deeper in water than the others.

On the other hand, in the sections without AuNPs, we observe that sodium ions are dissolved in the water at a level comparable to that of the AuNP-SDS, which is situated slightly further away.

## Conclusions

Through the study, CGMD was performed for a single and three AuNPs-SDS in an aqueous medium using MARTINI for 300 ns. Conducting analysis on Coulomb and van der Waals energy, diffusion, and structure. In the energy analysis, both systems showed an increase in energy with the rise in concentration, always accompanied by an attractive force. In the case of the Coulomb interaction between AuNPs and AuNPs, the concentrated system exhibited repulsion, which could be a factor to consider if the AuNP concentration increases considerably. These results indicate a trend that the AuNP-SDS CG model provides an acceptable framework for CG simulations alongside other structures. The diffusion analysis shows an increase in the diffusion coefficient with an increase in the AuNP-SDS numbers. The three AuNPs-SDS system display better diffusion in an aqueous medium than the single one, suggesting that introducing more nanoparticles forms a larger and more diffuse cluster. This property is desirable for substrates used to transport active ingredients. In the structural analysis, the RDF indicates that the ions, SDS, and AuNPs display the same structural order as the concentration increases. This suggests that the increase in concentration does not influence the organization of the beads in the SDS and that the AuNPs-SDS remain neutralized by sodium ions. The

Rg demonstrated a difference when we conducted the nucleus and the SDS for the single AuNP. As we anticipated, the Rg increased due to the flexibility of the ligands. However, no differences were observed among the three AuNPs regarding the nucleus and SDS; these last two exhibited the same Rg value. Therefore, regarding the stability of AuNPs, we conclude that both uncoated and coated particles interacting in an aqueous medium are stable and remain compact, highlighting their usefulness for particle transport in various study systems. The standard density reinforces the RDF analyses, where we can see the ions, SDS, and AuNP in a structural order. However, for the tree AuNPs system, we observe that one AuNP is slightly separated from the others. In this AuNP, the ion and the SDS were observed to be more separated from each other, suggesting that increasing concentration can change the way ions, SDS, and water interact in the same system. However, in this study, we can conclude that the three AuNP-SDS remain relatively close together instead of staying dispersed in the aqueous medium. The above opens a range of opportunities to design larger, organized structures that interact with one another or with other materials relevant to materials science.

*Acknowledgements*

The authors thank Diana J. Velásquez-Tinoco and Oscar V. Ortiz-Hernández for their time spent reading and offering comments on this work. Additionally, we would like to thank Alejandro J. Cuevas-Martínez for translating the draft article from Spanish to English.

## References

Abraham, M. J., Murtola, T., Schulz, R., Páll, S., Smith, J. C., Hess, B., & Lindah, E. (2015). Gromacs: High performance molecular simulations through multi-level parallelism from laptops to supercomputers. *SoftwareX*, *1–2*, 19–25. https://doi.org/10.1016/j.softx.2015.06.001

Abu Samah, N. H., & Heard, C. M. (2014). The effects of topically applied polyNIPAM-based nanogels and their monomers on skin cyclooxygenase expression, ex vivo. *Nanotoxicology*, *8*(1), 100–106. https://doi.org/10.3109/17435390.2012.754511

Albaladejo, S., Marqués, M. I., Scheffold, F., & Sáenz, J. J. (2009). Giant enhanced diffusion of gold nanoparticles in optical vortex fields. *Nano Letters*, *9*(10), 3527–3531. https://doi.org/10.1021/nl901745a

Alexander, S. T. (1986). The Method of Steepest Descent. *Adaptive Signal Processing*, 46–67. https://doi.org/10.1007/978-1-4612-4978-8_4

Applications, I. (2017). *Unique Roles of Gold Nanoparticles in Drug Delivery, Targeting and Imaging Applications*. https://doi.org/10.3390/molecules22091445

Asish, Pal; Aasheesh, S. S., & Bhattacharya. (2009). Role of Capping Ligands on the Nanoparticles in the Modulation of Properties of a Hybrid Matrix of Nanoparticles in a 2D Film and in a. 9169–9182. https://doi.org/10.1002/chem.200900304

Baranowska-Korczyc, A., Stelmach, E., Paterczyk, B., Maksymiuk, K., & Michalska, A. (2019). Ultrasmall self-assembly poly (N-isopropylacrylamide-butyl acrylate) (polyNIPAM-BA) thermoresponsive nanoparticles. Journal of Colloid and Interface Science, 542, 317–324. https://doi.org/10.1016/j.jcis.2019.02.004

Barrak, H., Saied, T., Chevallier, P., Laroche, G., Mnif, A., & Hamzaoui, A. H. (2016). Synthesis, characterization, and functionalization of ZnO nanoparticles by N-(trimethoxysilylpropyl) ethylenediamine triacetic acid (TMSEDTA): Investigation of the interactions between Phloroglucinol and ZnO@TMSEDTA. Arabian Journal of Chemistry. https://doi.org/10.1016/j.arabjc.2016.04.019

Baoukina, S., Rozmanov, D., & Tieleman, D. P. (2017). Composition Fluctuations in Lipid Bilayers. *Biophysical Journal*, *113*(12), 2750–2761. https://doi.org/10.1016/j.bpj.2017.10.009

Berendsen, H. J. C. (1991). Transport Properties Computed by Linear Response through Weak Coupling to a Bath. *Computer Simulation in Materials Science*, 139–155. https://doi.org/10.1007/978-94-011-3546-7_7

Bordoni, G. P., & Colherinhas, G. (2022). On the influence of increasing the concentration of Au144(SRCOO1-)60 nanoparticles in water/Na1+ solution using molecular dynamics simulations. *Journal of Molecular Liquids*, *368*, 120776. https://doi.org/10.1016/J.MOLLIQ.2022.120776

Bussi, G., Donadio, D., & Parrinello, M. (2007). Canonical sampling through velocity rescaling. *Journal of Chemical Physics*, *126*(1). https://doi.org/10.1063/1.2408420

Deshmukh, S., Mooney, D. A., McDermott, T., Kulkarni, S., & Don MacElroy, J. M. (2009). Molecular modeling of thermo-responsive hydrogels: Observation of lower critical solution temperature. *Soft Matter*, *5*(7), 1514–1521. https://doi.org/10.1039/b816443f

Elahi, N., Kamali, M., & Baghersad, M. H. (2018). Recent biomedical applications of gold nanoparticles: A review. *Talanta*, *184*(February), 537–556. https://doi.org/10.1016/j.talanta.2018.02.088

Estrada-López, E. D., Murce, E., Franca, M. P. P., & Pimentel, A. S. (2017). Prednisolone adsorption on lung surfactant models: Insights on the formation of nanoaggregates, monolayer collapse and prednisolone spreading. *RSC Advances*, *7*(9), 5272–5281. https://doi.org/10.1039/c6ra28422a

Fitzgerald, G., Dejoannis, J., & Meunier, M. (2015). Multiscale modeling of nanomaterials. In *Modeling, Characterization and Production of Nanomaterials: Electronics, Photonics and Energy Applications*. Elsevier Ltd. https://doi.org/10.1016/B978-1-78242-228-0.00001-6

Franco-ulloa, S., Riccardi, L., Rimembrana, F., Grottin, E., Pini, M., & Vivo, M. De. (2022). *NanoModeler CG: A Tool for Modeling and Engineering Functional Nanoparticles at a Coarse-Grained Resolution*. https://doi.org/10.1021/acs.jctc.2c01029

Ganesh, M., Hemalatha, P., Peng, M. M., & Jang, H. T. (2013). One pot synthesized Li, Zr doped porous silica nanoparticles for low temperature CO 2 adsorption. ARABIAN JOURNAL OF CHEMISTRY, 2–6. https://doi.org/10.1016/j.arabjc.2013.04.031

Gupta, R., & Rai, B. (2017). Effect of Size and Surface Charge of Gold Nanoparticles on their Skin Permeability: A Molecular Dynamics Study. *Scientific Reports*, *7*(February), 1–13. https://doi.org/10.1038/srep45292

Harding, G., & Harding, A. (2007). *X-ray Diffraction Imaging for Explosives Detection*. *October 2006*, 199–235.

Hockney, R. W., Goel, S. P., & Eastwood, J. W. (1974). Quite high-resolution computer models of plasma. *Journal of Computational Physics*, *14*(2), 148–158. https://doi.org/10.1016/0021-9991(74)90010-2

Hu, X., Zhang, Y., Ding, T., Liu, J., & Zhao, H. (2020). *Multifunctional Gold Nanoparticles: A Novel Nanomaterial for Various Medical Applications and Biological Activities*. *8*(August), 1–17. https://doi.org/10.3389/fbioe.2020.00990

Joshi, S. Y., & Deshmukh, S. A. (2021). A review of advancements in coarse-grained molecular dynamics simulations. *Molecular Simulation*, *47*(10–11), 786–803. https://doi.org/10.1080/08927022.2020.1828583

Khan, I., Saeed, K., & Khan, I. (2019). Nanoparticles: Properties, applications, and toxicities. *Arabian Journal of Chemistry*, *12*(7), 908–931. https://doi.org/10.1016/j.arabjc.2017.05.011

Khan, I., Yamani, Z. H., & Qurashi, A. (2017). Ultrasonics Sonochemistry Sonochemical-driven ultrafast facile synthesis of $SnO_2$ nanoparticles: Growth mechanism structural electrical and hydrogen gas sensing properties. Ultrasonics - Sonochemistry, 34, 484–490. https://doi.org/10.1016/j.ultsonch.2016.06.025

Kmiecik, S., Gront, D., Kolinski, M., Wieteska, L., Dawid, A. E., & Kolinski, A. (2016). Coarse-Grained Protein Models and Their Applications. Chemical Reviews, 116(14), 7898–7936. https://doi.org/10.1021/acs.chemrev.6b00163

Lee, J. I. E. U. N., Lee, N., Kim, T., Kim, J., & Hyeon, T. (2011). Multifunctional Mesoporous Silica Nanocomposite Nanoparticles for Theranostic Applications. 44(10), 893–902

Lu, X., Zhu, T., Chen, C., & Liu, Y. (2014). Right or Left: The Role of Nanoparticles in Pulmonary Diseases. 17577–17600. https://doi.org/10.3390/ijms151017577

Mansha, M., Khan, I., Ullah, N., & Qurashi, A. (2017). Synthesis, characterization, and hydrogen evolution reaction of carbazole-containing conjugated polymers. International Journal of Hydrogen Energy, 1–10. https://doi.org/10.1016/j.ijhydene.2017.02.053

Marrink, S. J., Risselada, H. J., Yefimov, S., Tieleman, D. P., & De Vries, A. H. (2007). The MARTINI force field: Coarse grained model for biomolecular simulations. *Journal of Physical Chemistry B*, *111*(27), 7812–7824. https://doi.org/10.1021/jp071097f

Marrink, S. J., & Tieleman, D. P. (2013). Perspective on the martini model. *Chemical Society Reviews*, *42*(16), 6801–6822. https://doi.org/10.1039/c3cs60093a

Marrink, S. J., Vries, A. H. De, & Mark, A. E. (2004). *Coarse Grained Model for Semiquantitative Lipid Simulations*. 750–760.

Montoya-Villegas, K., Navarro-Félix, R. ., Rejón-Garcia, L., Silva-Carillo, C., Trujillo-Navarrete, B., Lin-Ho, S. ., & Reynoso-Soto, E. . (2020). Synthesis of Au-$TiO_2$ nanoparticles as sensors of 3-mercaptopropionic acid. *Revista Mexicana De Ingenieria Quimica*, *19*(941–952), 97–104.

Núñez-Delgado, C., Luna-Flores, A., Conde-Hernández, L. A., Flores-Aquino, E., Romero-López, A., & Tepale, N. (2023). Biosynthesis of gold nanoparticles using the aqueous extract of *Hippocratea excelsa* root bark. Antioxidant and photocatalytic evaluation. Revista Mexicana De Ingeniería Química, 22(IA2367).

Owen, D. M. (2014). Methods in membrane lipids: Second edition. *Methods in Membrane Lipids: Second Edition*, *1232*, 1–327. https://doi.org/10.1007/978-1-4939-1752-5

Pizzirusso, A., De Nicola, A., & Milano, G. (2016). MARTINI Coarse-Grained Model of Triton TX-100 in Pure DPPC Monolayer and Bilayer Interfaces. *Journal of Physical Chemistry B*, *120*(16), 3821–3832. https://doi.org/10.1021/acs.jpcb.6b00646

Pronk, S., Páll, S., Schulz, R., Larsson, P., Bjelkmar, P., Apostolov, R., Shirts, M. R., Smith, J. C., Kasson, P. M., Van Der Spoel, D., Hess, B., & Lindahl, E. (2013). GROMACS 4.5: A high-throughput and highly parallel open-source molecular simulation toolkit. *Bioinformatics*, *29*(7), 845–854. https://doi.org/10.1093/bioinformatics/btt055

Ramacharyuly, P.V.R.K; Muhammad, Raeesh; Kumar, Praveen J.; Prasad, G. K. (2015). Iron Phthalocyanine Modified Mesoporous Titania Nanoparticles for Photocatalytic Activity and $CO_2$ Capture Applications. https://doi.org/10.1039/C5CP03576G

Ramalingam, V. (2019). Multifunctionality of gold nanoparticles: Plausible and convincing properties. *Advances in Colloid and Interface Science*, *271*, 101989. https://doi.org/10.1016/j.cis.2019.101989

Rawal, I., & Kaur, A. (2013). Sensors and Actuators A: Physical Synthesis of mesoporous polypyrrole nanowires / nanoparticles for ammonia gas sensing application. Sensors & Actuators: A. Physical, 203, 92–102. https://doi.org/10.1016/j.sna.2013.08.023

Shaalan, M., Saleh, M., & El-mahdy, M. (2016). Recent progress in applications of nanoparticles in fish medicine: A review. Nanomedicine: Nanotechnology, Biology, and Medicine, 12(3), 701–710. https://doi.org/10.1016/j.nano.2015.11.005

Si, K. J., Chen, Y., Shi, Q., & Cheng, W. (2018). Nanoparticle Superlattices: The Roles of Soft Ligands. https://doi.org/10.1002/advs.201700179

Souza, L. M. P., Nascimento, J. B., Romeu, A. L., Estrada-López, E. D., & Pimentel, A. S. (2018). Penetration of antimicrobial peptides in a lung surfactant model. *Colloids and Surfaces B: Biointerfaces*, *167*, 345–353. https://doi.org/10.1016/J.COLSURFB.2018.04.030

Taylor, P., Gunsteren, W. F. Van, & Berendsen, H. J. C. (2007). *A Leap-frog Algorithm for Stochastic Dynamics A LEAP-FROG ALGORITHM FOR STOCHASTIC DYNAMICS*. *May 2013*, 37–41.

Vaisey, G., Banerjee, P., North, A. J., Haselwandter, C. A., & Mackinnon, R. (2022). Piezo1 as a force-through-membrane sensor in red blood cells. *ELife*, *11*, 1–21. https://doi.org/10.7554/ELIFE.82621

Velasco-Rodríguez, V., Cornejo-Mazon, M., Flores-Flores, J. O., Gutierrez-Lopez, G. F., & Hernandez-Sanchez, H. (2012). Preparation and properties of alpha-lipoic acid-loaded chitosan nanoparticles. Revista Mexicana De Ingenieria Química, 11(1), 155–161.

Wassenaar, T. A., Ingólfsson, H. I., Böckmann, R. A., Tieleman, D. P., & Marrink, S. J. (2015). *Computational lipidomics with insane: a versatile tool for generating custom membranes for molecular simulations*. https://doi.org/10.1021/acs.jctc.5b00209

Wong, K., Chen, C., Wei, K., Roy, V. A. L., & Chathoth, S. M. (2015). Diffusion of gold nanoparticles in toluene and water as seen by dynamic light scattering. *Journal of Nanoparticle Research*, *17*(3). https://doi.org/10.1007/s11051-015-2965-x

Zimbone, M., Calcagno, L., Messina, G., Baeri, P., & Compagnini, G. (2011). Dynamic light scattering and UV-vis spectroscopy of gold nanoparticles solution. *Materials Letters*, *65*(19–20), 2906–2909. https://doi.org/10.1016/j.matlet.2011.06.054